International Journal of Heat and Mass Transfer 68 (2014) 383–390

Contents lists available at ScienceDirect

International Journal of Heat and Mass Transfer

journal homepage: www.elsevier.com/locate/ijhmt

Assessment of radiative heat transfer characteristics of a combustion mixture in a three-dimensional enclosure using RAD-NETT (with application to a fire resistance test furnace)

W.W. Yuen *, W.C. Tam, W.K. Chow

Department of Mechanical Engineering, The Hong Kong Polytechnic University, Hung Hom, Kowloon, Hong Kong, China

ARTICLE INFO

Article history:
Received 9 April 2013
Received in revised form 2 July 2013
Accepted 3 August 2013

Keywords:
RAD-NETT
Radiation heat transfer
Neural network
Fire resistance test furnace

ABSTRACT

Using RAD-NETT, a neural network correlation of the non-gray radiative absorption properties of combustion gases (CO_2 and H_2O) and soot, the emissivity and hemispherical absorptivity of a combustion mixture to a boundary in a rectangular enclosure is determined. Results show that the both the emissivity and hemispherical absorptivity have a strong dependence on the mixture properties, as well as the medium temperature and wall temperature. The gray assumption with emissivity equal to absorptivity is generally inaccurate. The numerical model is used to analyze temperature and heat transfer data generated from a fire resistance test furnace. Results show that emission and reflection from the wall boundaries have a major effect of the radiative heat flux measurement in a test sample in a fire resistance test. Numerical results also demonstrate that the furnace was operating essentially in an isothermal condition. From the perspective of a compartment fire, numerical data show that soot emission and emission from the wall are essential in the initiation of flashover in a compartment fire.

1. Introduction

In fire safety and other analyses of heat transfer in an absorbing and emitting combustion medium, the use of a constant emissivity and absorptivity is a common engineering approach because of the mathematical complexity to account for the non-gray and three-dimensional characteristics of radiative heat transfer. Over the years, a great deal of works have been reported in dealing with the non-gray multi-dimensional aspect of radiative heat transfer, particularly in a combustion media [1–4]. However, the proposed computational approaches are still not sufficiently efficient to eliminate the need to make this simplifying assumption in practical engineering system. Until now, there has been few direct assessment of this important engineering approximation in an actual three-dimensional combustion environment. In a recent work [5], a computationally efficient approach was developed for the evaluation of the total absorptivity of a one-dimensional slab of combustion mixture (CO_2, H_2O and soot) using narrow-band absorption data [6]. Specifically, numerical data for the total absorptivity, generated by a direct integration of the spectral data, are correlated by a neural network, RAD-NETT, as a function of the relevant physical parameters such as source temperature, absorption gas temperature, partial pressures and soot volume fraction. Based on RAD-NETT, the analysis of radiative heat transfer in a three-dimensional structure using realistic spectral data is now possible as the numerical integration needed for the evaluation the relevant surface–surface and surface-volume exchange factors can be done efficiently. Numerical data for these exchange factors can be further correlated by neural networks so that they can be implemented efficiently in an energy-balance zonal calculation. Results from such calculations can be used to demonstrate the radiative heat transfer characteristics of three-dimensional structures.

In the present work, the calculation is carried out to determine the radiative heat transfer in a specific rectangular enclosure. Numerical data are generated to assess quantitatively the effect of combustion parameters and geometry on the total emissivity and hemispherical absorptivity of the mixture. The commonly used engineering approximation of a gray combustion medium is assessed.

In fire safety, the use of a fire resistance test furnace to evaluate the "destructive potential" of building materials under standardized test conditions [7–9] is a commonly accepted practice to fulfill the various prescriptive and/or performance based fire resistance requirement. Since the "standard" required is "to expose building elements to heating in accordance with a standard temperature–

* Corresponding author.
E-mail address: yuen@engr.ucsb.edu (W.W. Yuen).

0017-9310/$ - see front matter © 2013 Published by Elsevier Ltd.
http://dx.doi.org/10.1016/j.ijheatmasstransfer.2013.08.009

Nomenclature

a_m^1	neural network parameter, Eq. (10)
A_1	area corresponds to the test specimen
A_i (I = 1, 6)	bounding areas of the fire resistance test furnace
b_m^1	neural network parameter
b^2	neural network parameter
c	constant defined by Eq. (6)
C_2	second radiation constant
dA_i (I = 1, 6)	differential areas
f_v	soot volume fraction
F_{CO_2}	fraction of CO_2 in gas mixture, Eq. (3)
$F_{w,i}$	heat flux due to emission from surface A_i
F_{ij}	view factor between surfaces A_i and A_j
L	line of sight distance between two integration areas
$L_{c,ij}$	characteristic length (center-to-center distance) between surfaces A_i and A_j
$L_{s,ij}$	mean beam length accounting for soot absorption
$L_{m,ij}$	mean beam length accounting for mixture absorption
n	real component of the index of fraction of soot
P_{CO_2}	partial pressure of CO_2
P_{H_2O}	partial pressure of H_2O
P_g	total partial pressure of the absorbing gas, Eq. (2)
$q_{inc,w,i}$	incident radiative flux due to emission from the ith wall, Eq. (24)
$q_{inc,w,i}$	incident radiative flux due to emission from all surrounding walls, Eq. (25)
$q_{inc,g}$	incident radiative flux due to emission from the mixture, Eq. (26)
q_{inc}	incident radiative flux due to emission from the mixture and walls, Eq. (27)
$q_{o,i}$	radiosity from surface A_i
$q_{og,i}$	radiosity from surface A_i due to mixture emission only
$R_{s,ij}$	ratio of soot mean beam length to characteristic length, Eq. (12)
S_iS_j	exchange factor, Eq. (1)
T_g	temperature of the combustion mixture
T_w	temperature of wall
W_m^1	neural network parameter
W_m^2	neural network parameter
X	dimension of the fire resistance test furnace
Y	dimension of the fire resistance test furnace
Z	dimension of the fire resistance test furnace
$\Delta\alpha$	difference between total absorptivity and soot absorptivity, Eq. (4)
α	total absorptivity of combustion mixture
α_s	absorptivity of soot, Eq. (5)
α_g	effective absorptivity of gas mixture, Eq. (23)
ε_g	effective emissivity of gas mixture, Eq. (21)
$\varepsilon_{w,i}$	emissivity of wall suface A_i
κ	complex component of the index of refraction
θ_i	angle between the line of sight and unit normal at dA_i
θ_j	angle between the line of sight and unit normal at dA_j
$\tau_{s,ij}$	optical thickness due to soot absorption, Eq. (13)

time relation" [9], there has been much uncertainty and controversy in relating results of the test to "real world fires", particularly under big fires [10]. For example, the heat load imposed on a test specimen depends strongly on the size of furnace, the conditions of the furnace wall and the nature of the combustion gases. Even when these test conditions are known, an effective heat transfer and radiation model is needed to relate the temperature–time history to the heat load on the test specimen. Modeling thus provides an important link between the test data and the actual "destructive potential" of the test specimen.

The fundamental understanding of the various heat transfer processes in a fire resistance test furnace was first reported more than 20 years ago [7,8]. Over the years, while there were some efforts to come up with different engineering approaches to better characterize the measured furnace data for design applications [11,12], very few efforts have been reported to provide further quantitative understanding of the fundamental heat transfer, in spite of the significance advances in the understanding of combustion, convective heat transfer and radiative heat transfer. A primary reason is the difficulty in simulating the realistic effect of radiation heat transfer in the combustion environment of the furnace. To account for the non-gray spectral absorption characteristics of the combustion products and the multi-dimensional effect of the furnace geometry, the computational effort is quite intensive and difficult to implement in a practical engineering calculation.

In the present work, the specific geometry of the rectangular enclosure is selected to be that of a full scale fire resistance test furnace for which some experimental data are available [13,14]. Numerical results will be compared directly with experimental data to illustrate the radiative heat transfer characteristics of a fire resistance test furnace. In addition, some general trend on the effect of radiative heat transfer on the initiation of flashover in a compartment fire is discussed.

2. Evaluation of emissivity and hemispherical absorptivity of a comustion mixture

2.1. Mathematical Formulation

A one-zone radiation heat transfer model is developed to determine the radiative heat flux incident on one of its boundary as a function of temperature, the nature of the combustion mixture and the geometry of the furnace. The volume is assumed to be a three dimensional rectangular enclosure with dimensions X, Y and Z as shown in Fig. 1.

Even in a one zone model in which the temperature and combustion conditions are assumed to be uniform in the furnace interior, radiative heat transfer is three-dimensional and the various exchange factors must be evaluated for the particular furnace geometry. Specifically, the exchange factor between two surfaces is given by

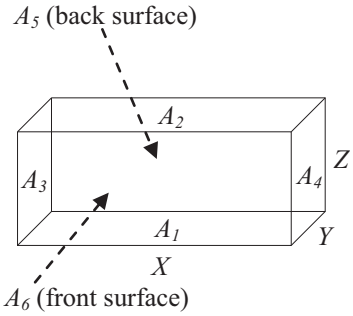

Fig. 1. The geometry and area identification used in the model for a fire resistance test furnace.

$$S_iS_j = \int_{A_i}\int_{A_j} \frac{\lfloor 1-\alpha(T_w,T_g,P_gL,F_{CO_2},f_vL)\rfloor \cos\theta_i\cos\theta_j}{\pi L^2} dA_i\,dA_j \quad (1)$$

In Eq. (1), L is the line-of-sight distance between the two integration area elements dA_i and dA_j. θ_i and θ_j are the angles between the line-of-sight and the unit normal vector of the two differential area elements. T_w is the temperature of the emitting wall and T_g the temperature of the absorbing gas. f_v is the soot volume fraction. P_g is the total partial pressure of the absorbing gas given by

$$P_g = P_{CO_2} + P_{H_2O} \quad (2)$$

with P_{CO_2} and P_{H_2O} being the partial pressure of CO_2 and H_2O respectively and

$$F_{CO_2} = \frac{P_{CO_2}}{P_g} \quad (3)$$

The total absorptivity, $\alpha(T_w,T_g,F_{CO_2},P_gL,f_vL)$, is evaluated along the line of sight between the two area elements. Utilizing the formulation of RAD-NETT, the total absorptivity is separated into two components as follow:

$$\alpha(T_w,T_g,P_gL,F_{CO_2},f_vL) = \Delta\alpha(T_w,T_g,P_gL,F_{CO_2},f_vL) + \alpha_s(T_w,f_vL) \quad (4)$$

$\alpha_s(T_w,f_vL)$ is the absorptivity due to soot absorption only and is given by

$$\alpha_s(T_w,f_vL) = 1 - \frac{15}{\pi^4}\psi^{(3)}\left(1+\frac{cLT_w}{C_2}\right) \quad (5)$$

with

$$c = 36\pi f_v \frac{n\kappa}{(n^2-\kappa^2+2)^2+4n^2\kappa^2} \quad (6)$$

C_2 is the second radiation constant and $\psi^{(3)}(z)$ is the pentagamma function. The added absorptivity, $\Delta\alpha(T_w,T_g,P_gL,F_{CO_2},f_vL)$, is correlated by a neural network over the following range of mixture properties

$$\begin{aligned} &0 \leqslant P_g \leqslant 100\ \text{kPa}\\ &0 \leqslant F_{CO_2} \leqslant 1.0\\ &0 \leqslant f_v \leqslant 1.0e-7\\ &400\ \text{K} \leqslant T_w,\quad T_g \leqslant 1400\ \text{K} \end{aligned} \quad (7)$$

with the total pressure of the furnace maintained at 100 kPa (1 atm).

While the exchange factor can be easily evaluated for a give geometry and mixture properties with the RAD-NETT correlation and a numerical integration, it is still computationally intensive in an actual engineering calculation in which the mixture properties and the wall temperature can be changing continuously. To facilitate a more efficient computational approach, the exchange factor is written as

$$S_iS_j = A_iF_{ij}\lfloor 1-\Delta\alpha(T_w,T_g,P_gL_{m,ij},F_{CO_2},f_vL_{m,ij}) - \alpha_{s,ij}(T_w,f_vL_{s,ij})\rfloor \quad (8)$$

where F_{ij} is the view factor between the two surfaces, and $L_{m,ij}$ and $L_{s,ij}$ are two "mean beam length" introduced to characterize the absorption by the soot $(\alpha_{s,ij}(T_w,f_vL_{s,ij}))$ and the gas mixture $(\Delta\alpha(T_w,T_g,P_gL_{m,ij},F_{CO_2},f_vL_{m,ij}))$ respectively. The concept of mean beam length was introduced originally to separate the effect of geometry from mixture properties on the evaluation of exchange factor [15]. While this separation works for some selective geometry and also in the limit of small optical thickness, the mean beam length is generally a function of both mixture properties and geometry [16]. Nevertheless, the influence of geometry on the mean beam length is expected to be less and it is therefore more efficient to develop correlations for mean beam lengths than for the exchange factors.

The development of neural networks for the different mean beam lengths is carried out for $(X,Y,Z) = (4\,\text{m}, 5\,\text{m}, 3\,\text{m})$. These dimensions are selected because they correspond to those of a full scale fire resistance test furnace for which experimental data for surface heat flux are available [13,14]. This will facilitate the interpretation of testing data which will be conducted in a later section.

For parallel surfaces, the three relevant mean beam lengths are demonstrated numerically to be independent of the mixture properties as follow:

$$\begin{aligned} L_{s,12} &= L_{m,12} = 1.165Z\\ L_{s,34} &= L_{m,34} = 1.1X\\ L_{s,56} &= L_{m,56} = 1.06Y \end{aligned} \quad (9)$$

For two surfaces which are perpendicular, both mean beam lengths depend strongly on the soot and mixture properties and they are tabulated over the range of properties as given by Eq. (7). The numerical data are then correlated by neural networks.

The soot mean beam lengths are correlated by a two-layer neural network as follow:

$$\tilde{R}_{L_{s,ij}} = \sum_{m=1}^{3} a_m^1 W_m^2 + b^2 \quad (10)$$

with

$$a_m^1 = \tanh\lfloor W_m^1\tilde{\tau}_{s,ij} + b_m^1\rfloor, \quad m = 1,3 \quad (11)$$

where

$$R_{L_{s,ij}} = \frac{L_{s,ij}}{L_{c,ij}} \quad (12)$$

and $\tau_{s,ij}$ is the soot optical thickness between the two surfaces given by

$$\tau_{s,ij} = \frac{cL_{c,ij}T}{C_2} \quad (13)$$

with $L_{c,ij}$, the characteristic length, is defined to be the center-to-center distance between the two surfaces. The symbol $\tilde{x}$ stands for the normalized value of the variable which takes on the value of 0 and 1 corresponded to the minimum and maximum value of the variable respectively. Numerical values of minimum and maximum value of the optical thickness and mean beam length, together with the network elements are given in Table 1.

For the mixture mean beam length, $L_{m,ij}$, numerical data show that for small mixture pressure-pathlength $(P_gL_{c,ij})$, the mean beam length is only a function of the mixture pressure-pathlength and independent of other mixture properties as shown in Fig. 2. For $P_gL_{c,ij} > 5$, the mean beam length depends strongly on the mixture properties and they are correlated by neural networks. In general, a three-layer network with dimensions similar to those used for RAD-NETT are needed for the correlation. Numerical data for the

Table 1
Neural network data for the soot mean beam length $L_{s,ij}$ for perpendicular surfaces in the fire resistance test furnace.

i	j	$\tau_{s,ij,\min}$ / $\tau_{s,ij,\max}$	$R_{L_{s,ij},\min}$ / $R_{L_{s,ij},\max}$	W^1	b^1	W^2	b^2
1,2	3,4	0.05	0.117	3.304	−5.078	−2.154	3.866
		20.0	0.795	1.671	2.107	−1.877	
				−9.814	−11.07	5.024	
1,2	5,6	0.05	0.112	3.235	−5.146	−2.909	3.183
		20.0	0.704	1.659	2.062	-1.825	
				−9.625	−10.91	5.145	
3,4	5,6	0.05	0.102	3.245	−5.140	−2.704	2.957
		20.0	0.685	1.623	1.967	−1.609	
				−8.926	−10.15	4.935	

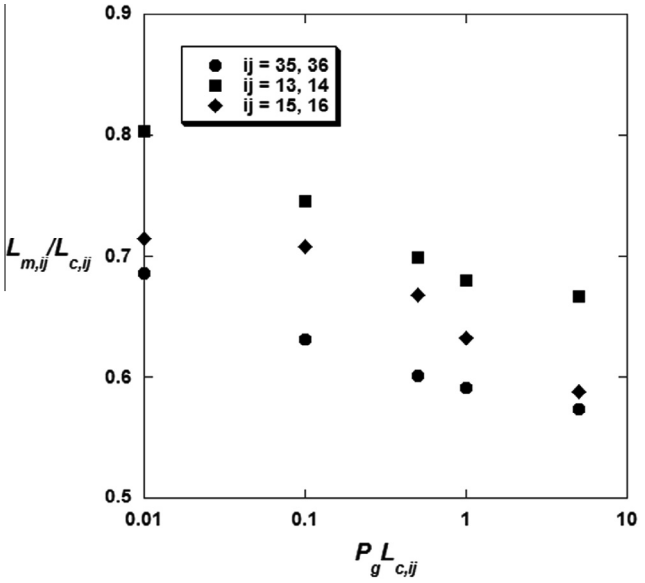

Fig. 2. The mixture mean beam length for perpendicular areas for the considered fire resistance test furnace for small and moderate mixture pressure-pathlengths.

networks are presented in a separate reference [17] and will be available upon request.

With the tabulated mean beam lengths, a zonal analysis is carried out to determine the radiative heat flux incident on the surfaces. Since the exchange factors depend both on the source temperature (T_w) and the medium (T_g), separate analyses are needed to determine the incident heat flux due to the emission from the different walls and that due to the gas mixture. Specifically, a zonal analysis is carried out for one hot wall (A_i), with emissivity ε_i, maintained at temperature $T_{w,i}$ while the remaining walls are assumed to be non-emitting ($T_{w,j} = 0, j \neq i$) with emissivity of ε_j. The mixture is assumed to be absorbing and non-emitting at temperature T_g. Assuming that all surfaces are diffuse, the relevant equations generated from the zonal analysis [18,20] are

$$\frac{(\sigma T_{w,i}^4 - q_{o,i})A_i\varepsilon_i}{(1-\varepsilon_i)} = A_i q_{o,i} - \sum_{k\neq i} S_i S_k (T_{w,i}, T_g) q_{o,k} \tag{14}$$

$$\frac{(-q_{o,j})A_j\varepsilon_j}{(1-\varepsilon_j)} = A_i q_{o,j} - \sum_{k\neq j} S_j S_k (T_{w,i}, T_g) q_{o,k}, \quad j \neq i \tag{15}$$

Note that in Eqs. (14) and (15), all the exchange factors are evaluated at a source temperature of $T_{w,i}$ and a medium temperature of T_g. The heat transfer to the different walls are given by

$$Q_i = \sum_{k\neq i} S_i S_k (T_{w,i}, T_g) q_{o,k} - A_i q_{o,i} \tag{16}$$

And the heat transfer into the absorbing and non-emitting medium is

$$Q_g = \sum_{i=1}^{6} \left[A_i - \sum_{j\neq i} S_i S_j (T_{w,i}, T_g) \right] q_{o,i} \tag{17}$$

To account for the mixture emission, another analysis is carried out for an absorbing and emitting mixture with reflecting but non-emitting walls. The relevant equations are

$$\frac{(-q_{og,i})A_i\varepsilon_i}{(1-\varepsilon_i)} = A_i q_{og,i} - \sum_{j\neq i} S_i S_j (T_g, T_g) q_{og,j} - \sum_{j\neq i} [A_i F_{ij} - S_i S_j (T_g, T_g)] \sigma T_g^4 \tag{18}$$

for all the absorbing, non-emitting wall ($i = 1, 6$). The heat transfer to the wall is now given by

$$Q_i = \sum_{k\neq i} S_i S_k (T_g, T_g) q_{og,k} - A_i q_{og,i} + [A_i - \sum_{j\neq i} S_i S_j (T_g, T_g)] \sigma T_g^4 \tag{19}$$

and the heat transfer to the medium is

$$Q_g = \sum_{i=1}^{6} \left[A_i - \sum_{j\neq i} S_i S_j (T_g, T_g) \right] [q_{og,i} - \sigma T_g^4] \tag{20}$$

With repeated application of Eqs. (14)–(17) to each surrounding emitting walls and together with Eqs. (18)–(20) for the emitting medium, the radiative heat transfer to the different walls and the medium for an enclosure with different boundary conditions and properties can be readily determined.

2.2. Radiative properties of a CO_2/H_2O/soot mixture

One of the important parameters which are of interest to the heat transfer community is the emissivity and absorptivity of the combustion medium. In reference [7], for example, it was suggested that for a fire resistance test furnace and based on "measurements made with a narrow-angle radiometer viewing the gas through a porthole against a water-cooled surface installed across the furnace", the effective absorption coefficient is estimated to be in the range of 0.18–0.22. For a characteristic length of 3 m, these data suggested an absorptivity in the range of 0.42–0.48. The current model provides an opportunity to assess this important property based on fundamental physics.

For a given set of mixture properties and temperature, the emissivity of the mixiture, radiating to the test specimen (area A_1) can be obtained from the solution to the analysis of an emitting medium and reflecting and non-emitting walls (Eq. (19)) as

$$\varepsilon_g = \frac{Q_1}{A_1 \sigma T_g^4} = \frac{1}{A_1}\left[1 - \sum_{j=2}^{6} S_1 S_j (T_g, T_g)\right] + \frac{1}{A_1 \sigma T_g^4} \sum_{j=2}^{6} [A_1 F_{1j} - S_1 S_j (T_g, T_g)] q_{og,j} \tag{21}$$

Note that the second term corresponds to the added emission to the test specimen due to the reflection of the surrounding walls. The concept of gas absorptivity, in general, depends on the direction and the orientation of the emitting surface. For a single emitting surface, A_i, with temperature $T_{w,i}$, solution to Eqs. (14)–(17) can be used to give

$$\alpha_{g,i}(T_{w,i}, T_g) = \frac{1}{A_1 F_{1i} \sigma T_{w,i}^4} \sum_{j=2}^{6} [A_1 F_{1j} - S_1 S_j (T_{w,i}, T_g)] q_{o,j} \tag{22}$$

The hemispherical absorptivity, $\alpha_g(T_w, T_g)$, which is generated by assuming all the surrounding wall are emitting at the same temperature T_w, is given by

$$\alpha_g(T_w, T_g) = \frac{1}{A_1} \sum_{j=2}^{6} A_1 F_{1j} \alpha_{g,j}(T_w, T_g) \tag{23}$$

For a typical gaseous concentration found in a combustion products ($P_{CO_2} = 5$ kPa, $P_{C_2O} = 5$ kPa), the emissivity of the mixture as a function of gas temperature and soot volume fraction with black surrounding wall is shown in Fig. 3. Both the mixture temperature and soot volume fraction have strong effect of the mixture emissivity. For the case with no soot, the qualitative effect of temperature on the emissivity is similar to that of a one-dimensional layer [19]. The slight nonlinearity in the region of 700 K corresponds to the effect of the strong CO_2 absorption band at 4.2 μm. It is interesting to observe that while the emissivity is generally

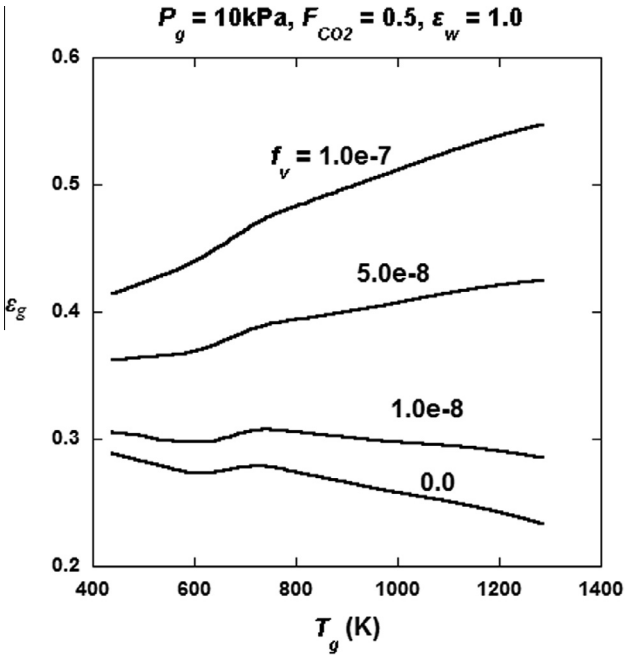

Fig. 3. The emissivity of the mixture for the considered fire resistance test furnace with black surrounding wall.

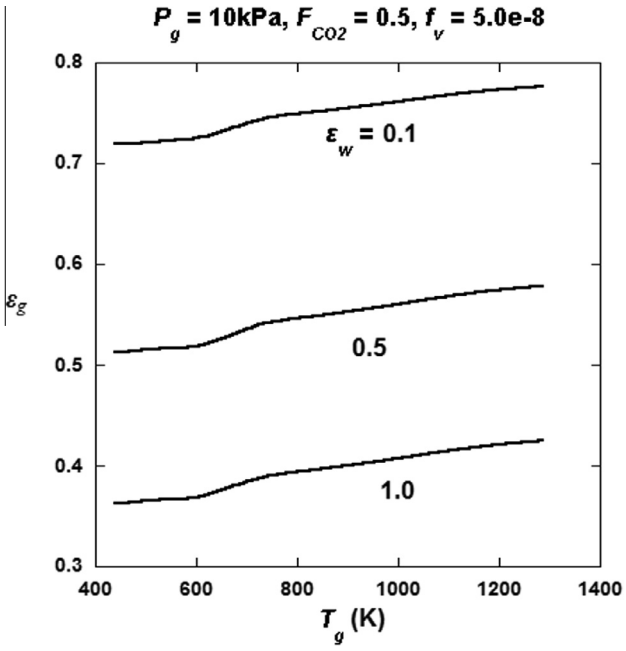

Fig. 4b. Effective of wall emissivity on the mixture emissivity in the considered fire resistance test furnace for a sooty mixture.

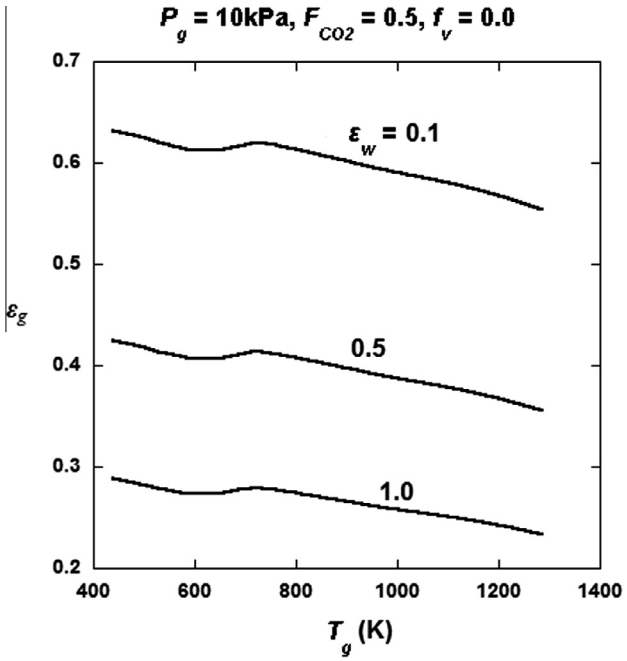

Fig. 4a. Effective of wall emissivity on the mixture emissivity in the considered fire resistance test furnace for a pure gas mixture.

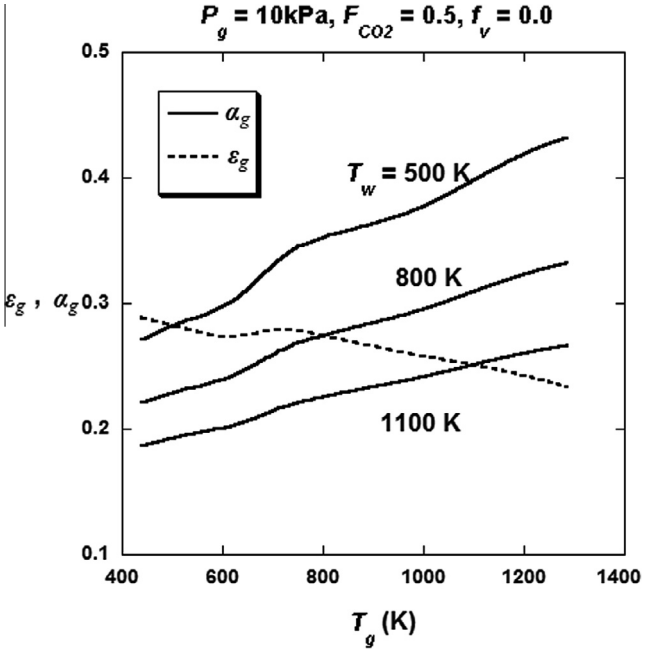

Fig. 5a. The absorptivity of the mixture for the considered fire resistance test furnace at different wall temperature (the emissivity of the mixture is also shown in the figure for comparison).

a decreasing function with gas temperature for a pure gas mixture ($f_v = 0$), it becomes an increasing function with temperature for a sooty mixture ($f_v > 5.e{-}8$).

The effect of wall reflectivity on the effective mixture emissivity is shown in Figs. 4(a) and 4(b). For simplicity, all surrounding walls are assumed to be at the same emissivity, ε_w, in the calculation for these data. As expected, the effective emissivity increases as the wall reflection increases.

It should be noted that as shown by data in Figs. 3, 4(a) and 4(b), the mixture emissivity is much less than unity even in the case of high soot concentration and high wall reflectivity. The assumption of a "black" combustion product mixture is therefore an idealization which is not supported by fundamental physics.

For a pure gas mixture, the hemispherical absorptivity as a function of wall temperature and mixture temperature is shown in Fig. 5(a). At different wall temperature, the hemispherical absorptivity decreases with increasing gas temperature, which is opposite to the trend for emissivity for a pure gas. The hemispherical absorptivity for a sooty mixture is shown in Fig. 5(b). The

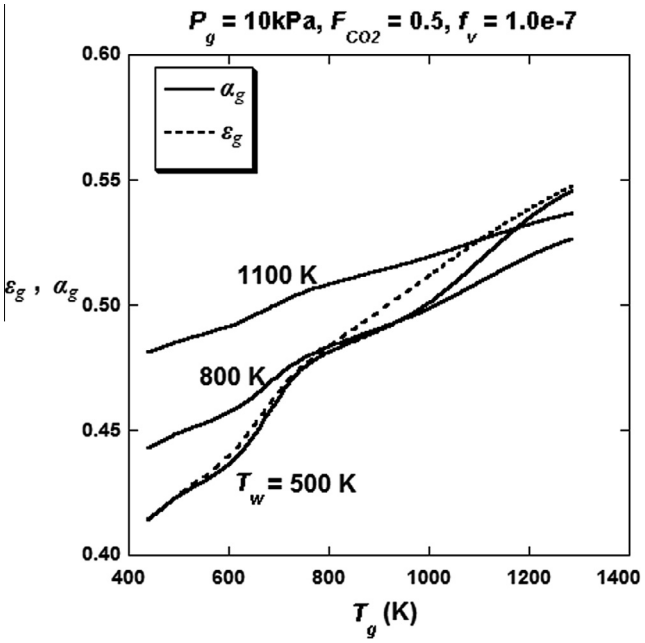

Fig. 5b. The absorptivity of a sooty mixture for the considered fire resistance test furnace at different wall temperature (the emissivity of the mixture is also shown in the figure for comparison).

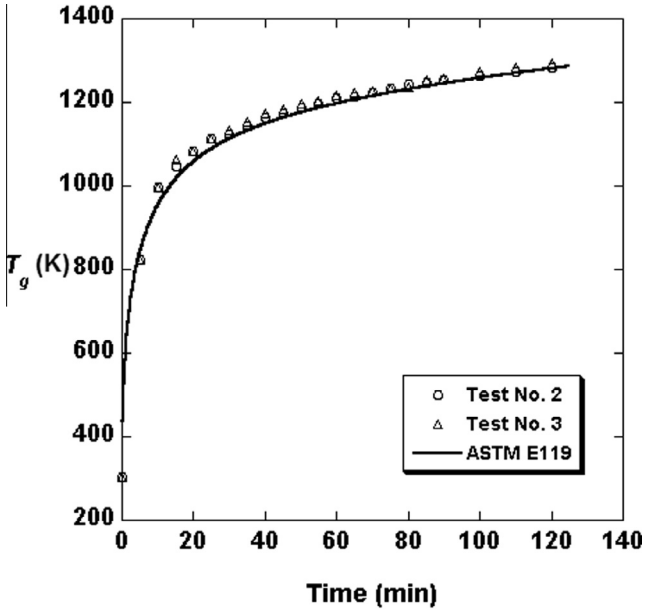

Fig. 6. Comparison between the measured furnace temperature and the ASTM E119 time–temperature curve used in the calculation.

hemispherical absorptivity for a sooty mixture increases with wall temperature, particularly in the region of low mixture temperature.

Comparison between the emissivity and hemispherical absorptivity demonstrates clearly that the two properties are different and have different dependence on combustion parameters. The assumption of a gray medium with constant and equal emissivity and hemispherical absorptivity for the combustion products is, therefore, not supported by fundamental physics.

3. Analysis of a fire resistance test furnace

A primary objective of a fire resistance test furnace is to determine the heat load on test specimen for a given combustion condition. In Refs. [13,14], for example, temperature and heat flux data were obtained from a full scale fire resistance test furnace (5 m × 4 m × 3 m) and also from an intermediate scale (1.2 m × 1.8 m × 0.5 m) in an attempt to resolve the difficult issue of scaling in fire resistance testing. Since full scale tests are time consuming and expensive, there are significant interest in performing small scale tests and utilizing the data for design and safety applications. Based on measured heat fluxes obtained from the two furnaces generated with the same time–temperature heating profile generated by a propone-fired combustion, it was concluded that the heat exposure in the intermediate-scale furnace is only slightly higher (15%) than in the full-scale furnace. The authors concluded that "For fire exposure, testing an assembly in an intermediate-scale furnace will provide a conservative performance compared to a full-scale furnace".

Even though the amount of quantitative data presented in Refs. [13,14] are limited (only furnace temperature and heat flux at the test specimen are presented), an analysis based on RAD-NETT can be used to provide a quantitative interpretation of the experimental data and to give an assessment of the relevant radiaitve heat transfer mechanisms in the furnace. In the experiment, the combustion within the furnace is controlled so that the measure furnace average temperature follow the ASTM E119 time–temperature curve [9] as shown in Fig. 6. Since it is difficult to determine the exact control mechanism to maintain the furnace temperature (e.g. the amount of fuel consumed by the combustion, the mixture conditions, etc.), it is not possible to do a complete simulation of the furnace performance based on first principle. The present work thus focuses only on the radiative heat transfer. Even though convection is expected to have an important contribution to the overall heat transfer [11,12], the radiation-only analysis can still be effective in illustrate some qualitative aspects of the heat transfer process.

A computer code, FRTF-RAD (Fire Resistance Testing Furnace with Radiation), is developed to determine the incident radiative heat flux on the test specimen. The code incorporates the zonal analysis presented in the previous section with all the neural network exchange factors. The mixture temperature history and the wall temperature history for all the enclosure boundaries except area A_1 are prescribed by the user as input conditions. Since the objective is to determine the incident heat flux on the test sample, the area A_1 is assumed to be a non-emitting but reflecting surface. Based on solution to Eqs. (14) and (15), the incident flux due to the emission from a single emitting wall can be generated from the radiosity from the different walls as

$$q_{Inc.,w,i}(T_{w,i},T_g)=\frac{1}{A_1}\sum_{j=2}^{6}S_1S_j(T_{w,i},T_g)q_{o,j} \tag{24}$$

The total incident flux due to emission from all the surrounding walls is given by

$$q_{Inc.,w}=\sum_{j=2}^{6}q_{Inc.,w,j}(T_{w,j},T_g) \tag{25}$$

The incident flux due to the mixture emission can be generated from the solution to Eq. (18) as

$$q_{Inc.,g}=\frac{1}{A_1}\sum_{k\neq1}S_1S_k(T_g,T_g)q_{og,k}+\left[1-\frac{1}{A_1}\sum_{j\neq1}S_iS_j(T_g,T_g)\right]\sigma T_g^4 \tag{26}$$

and the total incident radiative heat flux due to both wall and gas emission is given by

$$q_{inc}=q_{inc,w}+q_{inc,g} \tag{27}$$

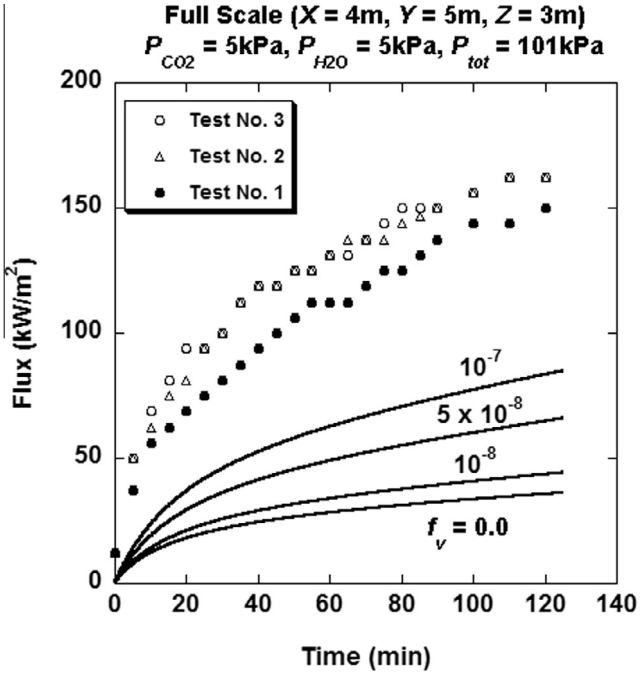

Fig. 7. Comparison between the measured heat flux to the test specimen at the full-scale fire resistance furnace and the predicted radiative heat flux from the emission of combustion products only.

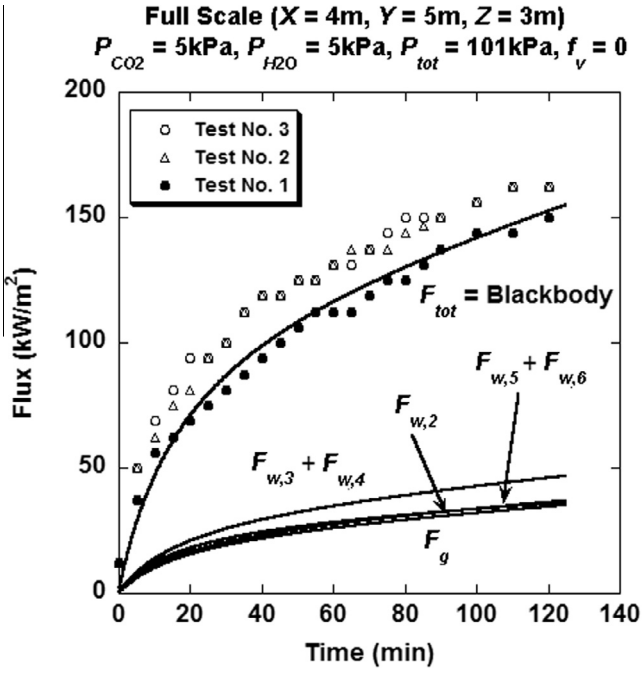

Fig. 8a. Prediction of heat flux from the different walls and the heat flux from the combustion mixture to the test specimen with $f_v = 0.0$. The wall temperature is assumed to be identical to the temperature of the mixture.

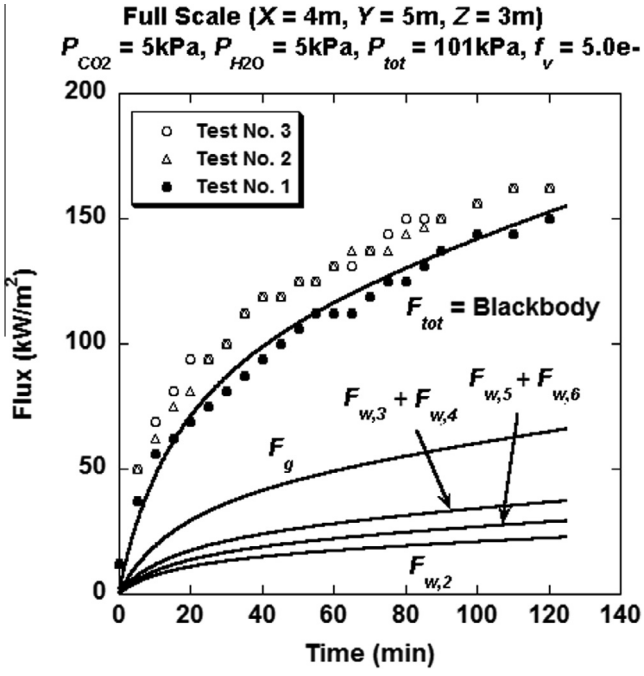

Fig. 8b. Prediction of heat flux from the different walls and the heat flux from the combustion mixture to the test specimen with $f_v = 5.0e{-}8$. The wall temperature is assumed to be identical to the temperature of the mixture.

Using the ASTM E119 time–temperature curve and assuming a moderate value of partial pressure (5 kPa) for H_2O and CO_2, the heat flux to the test specimen (A_1) generated by the combustion gas/soot mixture in the full scale furnace at various soot volume fraction, together with the experimental data from three independent repeated tests, are shown in Fig. 7. It is apparent that emission from the combustion gases/soot mixture is insufficient to generate the observed heat flux, even when the soot volume fraction is increased to physically unrealistic large values. These results suggest strongly that the radiation from the furnace wall contributes significantly to the total heat flux at the test specimen.

Thermodynamically, it can be shown that for an isothermal furnace with the furnace walls maintained at the same temperature as the combustion medium, the heat flux to the test specimen is a maximum and corresponds to that of a blackbody at the furnace temperature. The numerical data for an isothermal furnace, together with the measured heat flux, are presented in Figs. 8(a) and 8(b). The measured heat flux for all three cases follows the blackbody heat flux closely, suggesting that the furnace is indeed operating essentially at the isothermal condition. The slight increase in the measured temperature in tests 2 and 3 can probably attributed to convective heat transfer and the possibility that some portion of the walls might be at a temperature higher than the combustion temperature. Indeed, given that the heat exposure for both the full scale and intermediate scale furnace correspond closely to the blackbody heat flux (with the intermediate scale slightly higher) [13,14], the test results show that both furnaces are operating isothermally. The general conclusion that "an intermediate-scale furnace will provide a conservative performance compared to a full-scale furnace" reached in reference [13,14] is therefore applicable only for an isothermal furnace. Additional studies are required to understand the scalability of test results generated from non-isothermal furnaces.

4. Conclusion

Using RAD-NETT, a numerical model is developed to analyze the radiative heat transfer within a rectangular enclosure. For a three-dimensional rectangular enclosure, the general behavior of the emissivity and hemispherical absorptivity is demonstrated. The method is also applied to the analysis of radiative heat transfer in a fire resistance furnace. The success of the current work demonstrates that RAD-NETT, together with neural network, can be used

to developed efficient computational tool to provide realistic non-gray multi-dimensional radiative heat transfer analysis for practical engineering systems. These efforts will be pursued in future work.

References

[1] N. Lallemant, A. Sayre, R. Weber, Evaluation of emissivity correlations for $H_2O \pm CO_2 \pm N_2$/air mixtures and coupling with solution methods of the radiative transfer equation, Prog. Energy Combust. Sci. 22 (1996) 543–574.

[2] C.E. Choi, S.W. Baek, Numerical analysis of a spray combustion with non-gray radiation using weighted sum gray gases model, Combust. Sci. Technol. 115 (1996) 297–315.

[3] M.J. Yu, S.W. Baek, J.H. Park, An extension of the weighted sum of gray gases non-gray gas radiation model to a two phase mixture of non-gray gas with particles, Int. J. Heat Mass Transfer 43 (2000) 1699–1713.

[4] S. Mazumder, M. Modest, Application of the full spectrum correlated-k distribution approach to modeling non-gray radiation in combustion gases, Combust. Flame 129 (2002) 416–438.

[5] W.W. Yuen, RAD-NETT, a neural network based correlation developed for a realistic simulation of the non-gray radiative heat transfer effect in three-dimensional gas-particle mixture, Int. J. Heat Mass Transfer 52 (2009) 3159–3168.

[6] W.L. Grosshandler, RADCAL, A Narrow-Band Model for Radiation Calculations in a Combustion Environment, NIST-TN-1402, National Institute of Standard and Technology, 1993.

[7] T.Z. Harmathy, The fire resistance test and its relation to real-world fires, Fire Mater. 5 (3) (1981) 112–122.

[8] M.A. Sultan, T.Z. Harmathy, J.R. Mehaffey, Heat transmission in fire test furnaces, Fire Mater. 10 (1986) 47–55.

[9] ASTM E119-88, Standard Methods of Fire Tests of Building Construction and Materials, ASTM, Philadelphia, PA, 1995.

[10] W.K. Chow, J. Li, Are two 2-h fire rated shutters equivalent to a 4-h shutter using ASTM E119?, ASCE – J Architect. Eng. 15 (2) (2009) 67–70.

[11] U. Wickstrom, Adiabatic surface temperature and the plate thermometer for calculating heat transfer and controlling fire resistance furnaces, in: Proceedings of the Ninth International Symposium on Fire, Safety Science, 2008.

[12] U. Wickstrom, A. Robbins, G. Baker, The use of adiabatic surface temperature to design structure for fire exposure, J. Struct. Fire Eng. 2 (1) (2011) 21–28.

[13] M.A. Sultan, N.Benichou, B.Y. Min, Heat exposure in fire resistance furnaces: full-scale vs intermediate-scale, in: Proceedings of the 2003 Fire and Materials International Conference, San Francisco, CA, 2003, pp. 45–53.

[14] M.A. Sultan, Incident heat flux measurements in wall and floor furnaces of different sizes, Fire Mater. 30 (6) (2006) 383–396.

[15] H.C. Hottel, A.F. Sarofim, Radiative Transfer, McGraw Hill, New York, 1967.

[16] W.W. Yuen, Definition and evaluation of mean beam lengths for applications in multi-dimensional radiative heat transfer, a mathematically self-consistent approach, ASME J. Heat Transfer 130 (11) (2008) 114507.

[17] W.C. Tam, Analysis of heat transfer in a building structure accounting for the realistic effect of thermal radiation heat transfer, Ph.D. Thesis, the Hong Kong Polytechnic University, Hong Kong, China, 2013.

[18] R. Siegel, J.R. Howell, Thermal Radiation Heat Transfer, fourth ed., Taylor and Francis, New York, 2002.

[19] H.C. Hottel, Radiant heat transmission, in: William H. McAdams (Ed.), Heat Transmission, third ed., McGraw Hill, New York, 1954 (Ch. 4).

[20] W.W. Yuen, Development of a network analogy and evaluation of mean beam lengths for multi-dimensional absorbing/isotropically-scattering media, ASME J. Heat Transfer 112 (1990) 408–413.